File copy

INTERNAL DOCUMENT no. 292

IOS

DEACON LABORATORY

ARE/IOSDL Contract

"Studies in the Upper Ocean".

Summary Report for April 1985 - April 1990:

Phases I and II

by

A L New

[*This document should not be cited in a published bibliography, and is supplied for the use of the recipient only*].

Natural Environment Research Council

INSTITUTE OF OCEANOGRAPHIC SCIENCES DEACON LABORATORY

INSTITUTE OF OCEANOGRAPHIC SCIENCES

DEACON LABORATORY

Wormley, Godalming,
Surrey, GU8 5UB, U.K.

Telephone: 0428 79 4141
Telex: 858833 OCEANS G
Telefax: 0428 79 3066

DIRECTOR: Dr. C. P. Summerhayes

Natural Environment Research Council

Institute of Oceanographic Sciences Deacon Laboratory

Internal Document Number 292

ARE/IOSDL Contract "Studies in the Upper Ocean". Summary Report for April 1985 - April 1990: Phases I and II

by

A L New

DOCUMENT DATA SHEET

AUTHOR
A L New

PUBLICATION DATE 1990

TITLE

ARE/IOSDL Contract "Studies in the Upper Ocean".
Summary Report for April 1985 - April 1990: Phases I and II

REFERENCE

Institute of Oceanographic Sciences Deacon Laboratory Internal Document Number 292, 15pp + 14 figs.

ABSTRACT

This report summarises work under the ARE/IOSDL contract "Studies in the Upper Ocean". Work undertaken consisted essentially of a detailed study of the generation, propagation, and mixing effects of internal tides and internal waves in the Bay of Biscay, and involved a combination of in-situ observations with numerical modelling. Investigations of the upper ocean structure of the Iceland-Faeroes front, and the quality of Acoustic Doppler Current Profiler data on *RRS Discovery,* were also performed.

ISSUING ORGANISATION

Institute of Oceanographic Sciences
Deacon Laboratory
Wormley, Godalming
Surrey GU8 5UB. UK.

TELEPHONE 0428 79 4141

TELEX 858833 OCEANS G

TELEFAX 0428 79 3066

KEYWORDS

INTERNAL TIDES
INTERNAL WAVES
MIXING
BAY OF BISCAY
ICELAND-FAEROES FRONT
ACOUSTIC DOPPLER CURRENT PROFILER

CONTRACT
MoD
"Studies in the Upper Ocean"

PROJECT

PRICE

CONTENTS

1. Introduction

The overall objectives of this study have been to investigate processes determining the structure of the upper ocean, in particular the generation of internal tides and waves by steep shelf break topography, their subsequent propagation, and any mixing with which they may be associated.

The study was physically motivated by the observation that the shelf break in the Bay of Biscay is often associated with a region of cool water (see figure 1) and high phytoplankton abundance at the surface. Both these phenomena had been conjectured to result from physical mixing of the thermocline, resulting in the upwelling of cool water, rich in organic nutrients, to the well-illuminated surface layers, which would consequently provide a suitable environment for the growth of the phytoplankton (eg: see reference 4 in section 10). It had also been suggested that this mixing might result from internal waves of tidal period ("internal tides") which could be produced by the interaction of the surface tide with the steep shelf slope topography in the area. Further, it was thought that internal tides could cause large vertical displacements of the density structure, so that a knowledge of their form would be important for acoustic propagation and anti-submarine warfare.

These conjectures provided the initial motivation to develop a series of numerical models, and to undertake the collection of oceanographic data, as described in broad outline below. In addition, more recent research has centred on the analysis of fine-scale temperature data from the Iceland Faeroes frontal area, and on an investigation of the quality of Acoustic Doppler Current Profiler (ADCP) data collected on *RRS Discovery*.

2. Numerical models for internal tides

In order to generate large internal tides it is necessary that the topography be suitably steep (in the Bay of Biscay it is typically 1 in 10) and that the surface tides be sufficiently strong (reaching 0.8 ms^{-1} at Spring tides). It has been estimated by P G Baines (1982, Deep-Sea Research 29, 307-338) that the shelf break in the Biscay area (47-48^{o}N) is probably responsible for the most energetic tides anywhere in the world, and in order to investigate this more fully, and deduce whether mixing might result, it was necessary to develop numerical models.

Initially, a simple two-layer numerical model for long waves, following that of R D Pingree et al (1983, J Mar. Biol. Ass UK 64, 99-113) was programmed and applied to simple representative topography (ie a constant depth shelf and ocean, connected by a linear slope). Although it was inferred that internal tides might be responsible for the transport of significant quantities of sediment over the shelf break (references 1 and 7), the limitations of this type of model

for describing the propagation of internal tidal waves through a continuously stratified ocean were quickly realised.

For an ocean with a smoothly varying density profile in the vertical, $\rho_0(z)$, it can be shown that there are two dimensional internal modes of oscillation of the form

$$\eta(x, z, y) = a\,\Phi(z)\,e^{i(kx-\sigma t)} \tag{1}$$

for the vertical displacement of a fluid particle with mean position x, z and at time t, in which Φ satisfies the Taylor-Goldstein equation

$$\Phi_{zz} + k^2\left(\frac{N^2-\sigma^2}{\sigma^2-f^2}\right)\Phi = 0 \tag{2a}$$

$$\Phi(0) = \Phi(-h) = 0 \tag{2b}$$

where $N^2 = -g/\rho_0 \cdot \partial\rho_0/\partial z$, f is the coriolis frequency, σ is the frequency of the waves in question, and z = 0, -h correspond to the mean positions of the surface and horizontal bed respectively. This equation was solved, for density profiles typical of the Biscay region, by the technique of T H Bell (1971, NRL Report no 7294), to reveal the possible vertical structures ($\Phi(z)$), phase speeds ($c = \sigma/k$) and wavelengths ($\lambda = 2\pi/k$) of internal tides both on the shelf and in the ocean (mode n having n interior maxima of Φ)

For a two-dimensional topography consisting of uniform depth shelf and ocean regions connected by a linear slope, a numerical model was then constructed, similar to that of S J Prinsenberg and M Rattray (1975, Deep-Sea Research 22, 251-263), by assuming that the solution both over the shelf and in the ocean was described by sums of shelf and ocean modes respectively (ie solutions of equation (2) for shelf and ocean depths). The unknown amplitudes of these modes were then found essentially by solving the boundary conditions on the shelf slope, and full details are described in reference 8.

This model predicts the propagation of internal tidal energy along certain 'ray' paths emanating from the point of the shelf break which have the characteristic slope

$$\frac{dz}{dx} = \pm\left(\frac{\sigma^2 - f^2}{N^2 - \sigma^2}\right)^{1/2} \tag{3}$$

as shown in figure 2. By writing the displacement field as

$$\eta(x, z, y) = |\hat{\eta}|\cos(\sigma t - \Theta) \tag{4}$$

the rays are here revealed as regions of large amplitude oscillations and relatively rapid changes of phase. Note that the rays reflect from the sea-bed and then continue back up to the surface (at about 150 km from the shelf break) where, theoretically, they would give rise to large oscillations of the thermocline, and, after a second reflection, return to the abyssal depths

3. Internal tides near the thermocline

In September 1985, a cruise was undertaken with R D Pingree in order to investigate internal tides near the thermocline with the SeaSoar package (a towed cycling CTD). A typical example, in deep water, of isopycnals from this instrument is shown in figure 3 and three internal tidal depressions are in evidence (and also a number of higher frequency internal waves - see later discussion).

The wavelength of these depressions was observed to be about 45-50 km (in the deep ocean), and by solving the Taylor-Goldstein equation for the various modes, it was deduced that the summer thermocline was, unexpectedly, dominated by internal tides of modes 3 and/or 4 since these had about the correct wavelength. By contrast, the shelf motion was dominated by mode 1. These findings are summarised in reference 4.

In order to begin to understand why this should be so, a simple problem was solved analytically (unpublished work). By assuming the shelf slope to be vertical and the motion on the shelf to be effectively produced by a 'piston' (ie no vertical structure), it proved possible to solve for the amplitudes of the modes in the ocean without recourse to a computer model, and it was indeed found that the thermocline was dominated by mode 3, and that this was because the horizontal velocity structure of this mode most closely resembled that of the 'piston' forcing.

In order to incorporate a sloping shelf, and vertical structure on the shelf, however, the numerical model was set up as described above, and solved for a representative density profile and topography. By analysing the results from the model (see reference 8), it was again found that the thermocline motion was dominated by a mode 3 in the ocean and a mode 1 on the shelf, and further, that good agreement was obtained with the positions of internal tidal troughs observed with the SeaSoar, as shown in figure 4.

4. Internal tidal rays

Beams of energy travelling along characteristic ray paths in stratified fluids have been observed in the laboratory, but never before in nature. In order to investigate this phenomenon, and to provide a stringent test of the numerical model, a cruise was undertaken in September 1987. A number of tidal-period CTD stations were maintained spanning the shelf break, together with moorings, as shown in figure 5, and these were used to infer vertical profiles of oscillation amplitude and phase. A typical example is shown in figure 6, together with results from the numerical model. Overall, the agreement is extremely encouraging, with a definite maximum in the observed amplitude

at about the correct position for the ray (750 m in this example), and phases closely in line with those predicted by the model. The observed ray is somewhat broader in vertical extent, and contains smaller amplitudes, than that in the model, which may result from the dissipation and spreading of energy as the beam travels downwards, or from the finite width of the generation region (only a point in the model).

Figure 7 then summarises the results of this survey by showing sections (for clarity) of the amplitude profiles near the expected ray positions, and all the stations show a local maximum. The positions of these maxima follow a downward trend which is in close agreement with the theoretical ray position. This is described more fully in reference 13.

This is the first observational evidence that beams of energy actually occur in nature, and shows that, near the downward propagating ray, internal tidal amplitudes may often exceed 100 m. The effect of this on the propagation of sound through the ocean needs to be assessed.

More recent work of a similar nature has extended these results out to about 65 km from the shelf break, just beyond the point of the reflection of the ray from the sea-bed, as summarised in figures 8(a) and (b). In particular, the phase of the maximum elevation at the ray position was observed to be almost constant (at about -3 hours before High Water at Plymouth, HWP) from the shelf break to the point of bottom reflection, shortly after which a phase change of +4.3 hours was seen. This is in close agreement with results from the numerical model, which predicts a full phase change of +6.2 hours when the ray is sufficiently far from the bottom reflection.

5. Mixing near the shelf break

The numerical model predicts energy travelling upward from the shelf break as well as downwards into the ocean. It is interesting to conjecture that this was not observed in the above survey because of the production of mixing near the thermocline.

To investigate the possibility of mixing in the model, it is necessary to consider the Richardson number

$$R_i = N^2(z) / \left(\left(\frac{du}{dz}\right)^2 + \left(\frac{dv}{dz}\right)^2 \right) \qquad (5)$$

where (u, v) are the horizontal components of velocity. (A detailed study of internal tidal velocities in the model was made (reference 5), and good agreement with observations was obtained.) When $R_i < {}^1/_4$, we may expect the growth of instabilities and, if these become large enough, overturning and mixing may result. An investigation of linear stability theory was made in order to estimate

$$\gamma = \log_{10}(a_f / a_0) \qquad (6)$$

the logarithm of the amount by which a disturbance, of initial amplitude a_o, would grow (ie a_f is its final amplitude), and full details are given in reference 8. It was conjectured that mixing might result if γ exceeded 5 or 6. Figure 9 shows contours of R_i (summer stratification, spring tides) and values of γ, and reveals two regions of subcritical R_i (ie $R_i < 1/4$), as the upward propagating rays pass through the thermocline, in which mixing might occur.

These predicted mixing regions would then be expected to produce upwelling of cool water (and nutrients) to the surface layers. This was investigated during the September 1987 cruise with the novel IOSDL towed thermistor spar (see figure 10 and reference 11). Suspended from a catamaran towed at 2 ms^{-1} ahead of the ship's bow wake, the 9 m long spar supported 12 high resolution thermistors which sampled at 4 Hz. The results, figure 11, at Spring tides, show two zones of generally cool near-surface water closely aligned with the regions of mixing predicted by the model, relatively narrow bands near the surface reflections of the rays in which the temperatures are dramatically cooler (by 1-2 °C) than the surrounding waters, and that these bands are associated with small-scale temperature structures. Consequently, these observations strongly suggest the upward mixing of cooler deeper water into the near-surface layers, and support the hypothesis that internal tidal mixing is occurring as conjectured.

A paper presented at a conference (reference 10) describing this work was jointly awarded the Norman Heaps Prize for the best talk by a young scientist.

6. Higher frequency internal waves

As shown in figure 3, higher-frequency internal waves (20-40 minute periods) are evident in the upper layers of the ocean, and seem to occur with largest amplitudes near the internal tidal troughs, as though some form of trapping mechanism was operative.

An initial investigation of this problem involved the solution of the Taylor-Goldstein equation with a background shear U(z) included:

$$\emptyset_{zz} + \left(\frac{N^2}{(U-c)^2} - \frac{U_{zz}}{(U-c)} - k^2 \right) \emptyset = 0 \qquad (7)$$

where c is the phase speed of the internal waves. The shear U(z) was taken as that occurring in the crest or trough of an internal tide of mode 3 (which dominates the summer thermocline as described above), and the equation was solved for these two cases to yield the phase speeds of the higher frequency internal waves. In this way it was possible to estimate the periods of those waves which would be effectively trapped by, and travel along with, the same phase speed as the internal tide (ie at 1.3 ms^{-1}). This model gave predicted periods (seen from a ship moving at 8 kt) of 7 and 12 minutes for the internal waves in the trough and crest of the internal tide respectively, as compared with the 8

and 11 minutes which were actually observed. This agreement was taken as indicating that the waves were indeed effectively trapped by the tides.

It was consequently thought likely that the internal waves would result from steepening and dispersion of the internal tides, much as in the formation of undular bores. In order to investigate this, a weakly nonlinear, weakly dispersive equation with the effects of the earth's rotation (f) included was derived, and yielded

$$A_{tt} + f^2 A = c_o^2 A_{xx} + Er(A^2)_{xx} + D\,s\,A_{xxxx} \qquad (8)$$

as the evolution equation for the internal wave amplitude A. (Here c_o is the speed of the linear wave and E, r, D , s are defined parameters.) This has never before been investigated, and it is planned to solve this equation on the computer.

The current structure in the packets of these higher-frequency internal waves (often called 'solitary waves' or 'solitons') was investigated with the Acoustic Doppler Profiler on a cruise in July 1988. While the ship maintained station at about 150 km from the shelf break, two packets of extremely large solitons were detected, associated with internal tidal troughs, and both horizontal and vertical velocities were measured, as shown in figure 12. Horizontal currents rapidly increasing from zero to over 60 cm s^{-1}, and vertical velocities over 16 cm s^{-1} were recorded. In addition, a simultaneous XBT survey provided good resolution of the isotherm displacements during the passage of the solitons. The observed vertical velocities are entirely consistent with the vertical displacements observed in the XBT survey, are coherent in depth, and in phase with the solitons. As such, they are believed to be amongst the first reliable direct measurements of vertical currents in oceanic internal waves. More details are given in reference 16, where is is conjectured that internal waves as large as this and so far from any topography may have resulted from the beam of internal tidal energy again being near the sea surface and producing large oscillations there, as described above.

7. Upper ocean structure of the Iceland-Faeroes Front

More recently, research has broadened to include other processes and phenomena, which are described here and in the next section.

In 1988 a survey of the Iceland-Faeroes front was undertaken with the IOSDL thermistor spar. This allowed small-scale thermal structures to be investigated and in particular enabled estimates of the vertical turbulent heat flux to be made. Preliminary results from the analysis of this data indicate that the horizontal and vertical temperature gradients, and levels of the turbulent heat flux, which is always a maximum at the frontal position, decrease with distance to the East. The overall picture is consistent with the water masses (warm North Atlantic water, moving North, and colder Norwegian Sea water, moving South) meeting at the Western end of the front, where the gradients and mixing

between them is most intense, and of the front becoming gradually more diffuse with advection distance to the East, with continued, but decreasing, mixing at the frontal position. Typically, temperature changes of several degrees in only 200-400 m horizontally may be observed at the frontal position, with isotherm slopes of 1 in 20 to 1 in 5, and examples of data collected from two regions of the front are shown in figure 13 to illustrate its changing nature. This work relates to references 12 and 15.

8. The quality of Acoustic Doppler Current Profiler Data on RRS Discovery

Acoustic Doppler Current Profilers (ADCPs) are now important research tools which are commonplace on many ships, and data collected by these instruments is central to the understanding of several upper ocean processes. It is therefore important to have confidence in the quality of the resulting measurements. During RRS Discovery cruise 181, April 1989, the presence of a large spurious shear aligned with the direction of the ship's motion was noted on the ship's ADCP, and seemed to be particularly large when the ship was steaming into heavy seas. It is thought that this shear results from the trapping of bubbles produced by the bow wake and bow thruster, near to the ship's hull. Parameters representing the state of the wind and sea, and the ship's motion, were combined in such a way as to produce a function E, which estimates the severity of this effect, and so gives insight into the conditions under which large shears might be expected. The results were compared with data from Discovery cruise 164, January 1987, upon which the ADCP transducers (retracted into the ship's hull on cruise 181) were extended beyond the bubble layer, as illustrated in figure 14. The estimating function allows a meaningful intercomparison to be undertaken for the different weather conditions on the two cruises, and shows that the spurious shear may be effectively eliminated by extending the transducers. Spurious shear, caused by bubbles, seems to be a serious problem affecting the ADCPs on many ships, and every effort should be made to allow the transducers to be mounted clear of the hull. The function E, or similar, may be useful in assessing the severity of this effect for different ships.

A detailed description of E is beyond the scope of the present report, but further details are obtainable from the author, and will be written up for publication shortly.

9. Conclusions and possible future work

A detailed examination has been made of the generation, propagation and dissipation of internal tides and waves in the Bay of Biscay, both through the development of models and the collection of data, and significant progress has been made as outlined above. In particular, we believe we have provided the first ever direct observations of a beam of internal tidal energy propagating along the theoretical pathways from the shelf break, have described the nature and structure of the

internal tides and waves near the surface, and demonstrated that these motions appear to be responsible for significant mixing of the water column near the shelf break. Throughout this work, all the observations have been compared with, and interpreted in the light of, results from a numerical model, with which encouraging agreement has been attained. This has provided confidence both in the model and in our interpretations. The probable reason for the success of this work is the energetic nature of the internal tides in the Bay of Biscay, which are probably among the most powerful anywhere in the world. The importance of these phenomena and processes on the propagation of sound and for tactical exploitation in the South-West approaches needs to be fully assessed.

More recently, work has been involved with studies of fronts, eddies and potential vorticity (see references 18, 19), assessing the quality of data from shipborne Acoustic Doppler Current Profilers, which are important tools for understanding many upper ocean processes (reference 14), and also with an investigation of small scale temperature structures in the Iceland Faeroes front, an area of prime importance to MoD, based on data collected with the IOSDL towed thermistor spar (reference 15). This data is complementary to that collected by ARE's own thermistor chain on the same cruise (IF88) and should be compared with it. Under a possible extension to this contract (phase III) it has been proposed that this investigation should be completed, and that data from two further cruises (to be undertaken in 1990) should be analysed. The first of these cruises, in the North East Atlantic, would enhance our knowledge of internal tides and waves in the oceans, the second would provide a detailed survey of the Iceland-Faeroes front.

10. Papers and reports published under contract

1. Edwards, P.D., New, A.L. & Heathershaw, A.D., 1984. A numerical study of the internal tide at the Continental shelf-break. Institute of Oceanographic Sciences Internal Document No.222.

2. New, A.L., 1986b. Internal tides and waves in the Bay of Biscay. p.69 in: UK Oceanography '86, abstract only. Proceedings of Challenger Society conference, Southampton, 14-19 September 1986. 94pp.

3. New, A.L., 1986c. Internal tidal motions in the Bay of Biscay. (Abstract only). EOS, Transactions, American Geophysical Union, 68, 99.

4. Pingree, R.D., Mardell, G.T. & New, A.L., 1986. Propagation of internal tides from the upper slopes of the Bay of Biscay. Nature 321, 154-158.

5. New, A.L., 1987a. Internal tidal currents in the Bay of Biscay. Advances in Underwater Technology, Ocean Science and Offshore Engineering, 12, 279-293.

6. New, A.L., 1987b. An introduction to the RDI Acoustic Doppler Current Profiler as used on Challenger Cruise 15. Institute of Oceanographic Sciences Deacon Laboratory Internal Document No.272.

7. Heathershaw, A.D., New, A.L. & Edwards, P.D., 1987. Internal tides and sediment transport at the shelf-break in the Celtic Sea. Continental Shelf Research, 7, 485-517.

8. New, A.L., 1988a. Internal tidal mixing in the Bay of Biscay. Deep-Sea Research 35, 691-709.

9. New, A.L., 1988b. p.436 in: Forum - Turbulence at the shelf break. Journal of Navigation,41 (3), 434-439.

10. New, A.L., 1988c. Internal tides and mixing in the Bay of Biscay. In: UK Oceanography '88, abstract only. Proceedings of Challenger Society conference, Norwich, 11-16 September 1988.

11. Brandon, M.A., New, A.L. & Hall, A.J., 1988. The IOSDL towed thermistor spar on Challenger Cruise 18, September 1987. Institute of Oceanographic Sciences Deacon Laboratory Internal Document No.280.

12. Mohan, G.J., Hall, A.J. & New, A.L., 1989. The IOSDL towed thermistor spar on MV Sea Searcher in the Iceland Faeroes region, April/May 1988. Institute of Oceanographic Sciences Deacon Laboratory Internal Document No.285.

13. Pingree, R.D. & New, A.L., 1989. Downward propagation of internal tidal energy into the Bay of Biscay. Deep-Sea Research, 36, 736-758.

14. New, A.L., 1990a. Factors affecting the performance of the ADCP on R.R.S. Discovery. In: book of abstracts for Second European ADCP Workshop, 5 March, 1990, Institute of Oceanographic Sciences Deacon Laboratory,U.K.

15. New, A.L., 1990b. Upper ocean structure of the Iceland-Faeroes front. Annales Geophysicae, 1990 - Special Issue: XV General Assembly, Copenhagen, 23-27 April 1990, pp. 211-212. (Abstract only).

16. New, A.L. & Pingree, R.D., 1990a. Large-amplitude internal soliton packets in the central Bay of Biscay. Deep-Sea Research, 37, 513-524..

17. New, A.L. & Pingree, R.D., 1990b. Evidence for internal tidal mixing near the shelf break in the Bay of Biscay. Accepted in Deep-Sea Research.

18. Pollard, R.T. & New, A.L. 1990. Fronts and vertical circulation. In: book of abstracts for Undersea Defence Technology Conference, 7-9 February, 1990,Novotel, London.

19. Pollard, R.T., New, A.L. & Read, J.R., 1990. What can we learn from vorticity? Part 2 of W.O.C.E. Surface Layer Scientific Panel report, in press.

20. Rice, A.L., Thurston, M.H. & New, A.L., 1990. Dense aggregations of a hexactinellid sponge, Pheronema carpenteri, in the Porcupine Seabight (northeast Atlantic Ocean). Accepted in Progress in Oceanography.

Figure Captions

Fig 1 Chart of the Bay of Biscay, showing the study area for the 1985 survey (rectangle), mean sea-surface temperature contours (^{o}C), positions of internal tidal troughs 21-23 (see fig 3), and position B (see fig 9).

Fig 2 Profiles of amplitudes $|\hat{\eta}|$ (solid lines) and phases Θ (broken lines) in the numerical model (winter stratification and spring tides). The vertical lines coincide with the zeroes of the plotted quantities, and the scales are shown in the top right. The chained lines are the ray paths from the shelf break.

Fig 3 Example of SeaSoar tow on 19.9.85 showing internal tides (troughs 21-23 indicated, see fig 1) and waves. The isopycnals are at densities of 1026, 1026.5 and 1027 kg m^{-3}.

Fig 4 Internal tidal trough positions observed in the 1985 survey (o) and predicted by the model (x). The axes represent computational time and distance (shelf break at 2.9 km, positive distance into the ocean), and the broken lines show mode 1 and mode 3 propagation onto the shelf and into the ocean respectively.

Fig 5 Topography and positions of CTD stations (1,2,3,4,5,18) and moorings (110 and 111). The shaded area shows the estimated generation region for the internal tides (see reference 13).

Fig 6 Profiles of internal tidal amplitude and phase at CTD station 18 from 0600 GMT to 1700 GMT, 23.9.87 (bold lines), and numerical model results (thin lines).

Fig 7 Summary of internal tidal oscillations from the 1987 survey. Vertical lines are station positions, and the amplitude profiles (100 m scale indicated) near the ray path are illustrated (bold lines). The depths of amplitude maxima are plotted as bold dots and the dashed line is a ray path passing closely through these positions. The ray path predicted by the model is shown dotted. The actual (bold line) and model (shaded) topographies are also indicated. The upper axis is labelled with station numbers.

Fig. 8 (a) Diagram showing the theoretical ray path (chained line) for a beam of internal tidal energy at the M2 tidal frequency emanating from the critical depth (385m) on the upper slopes in the Bay of Biscay. Also shown is a summary of the internal tidal oscillations obtained during cruises in 1988 and 1987. Vertical lines represent mooring and CTD station positions and are identified with numbers. CTD stations 5 and 6 and mooring 116 are from the 1988 cruise, whereas moorings 110 and 111 and CTD 19 were obtained in 1987. The depth of the maxium amplitude of the internal tidal oscillation found at each station is plotted as an open circle and the range where the amplitude is more than 70% of the maximum value is indicated by the arrows. Two further rays are shown (solid lines) passing approximately through the 70% limits near mooring 110. The phase of the maximum upward displacement is given in hours with respect to High Water at Plymouth (HWP). A ray at the M2 tidal frequency would intersect mooring 116 at the depth marked M2; S2 is the corresponding point for a ray at the S2 tidal frequency. The topography is depicted by the bold line and is critical at 385m; the horizontal distance scale is measured from the critical point.
(b) Numerical model (see reference 8) phases (hours after HWP) near the main, initially downward-propagating ray path (broken line). The model topography is also shown.

Fig 9 Contours (at values of 10, 1 and $^1/_4$) of the minimum Richardson numbers (over a tidal cyde) predicted by the model (summer stratification and spring tides). The broken lines are the ray paths and the values of γ at particular positions along these paths are indicated.

Fig. 10. The IOSDL towed thermistor spar (description in text). The thermistors were set at depths below the mean water line of 0.81, 1.41, 1.91, 2.41, 2.91, 3.91, 4.65, 5.15, 5.65, 6.65, 7.65 and 8.65 m.

Fig. 11. (a) Thermistor spar record near Spring tides, showing 10-second averaged data. The temperature scale (°C) is correct for the uppermost trace, corresponding to the highest thermistor on the spar, and successive traces are taken from successive thermistors down the spar, each being successively offset by 0.75°C. X (km) represents distance in the numerical model. (b) Contours of 'instantaneous' Richardson number predicted by the numerical model (continuous lines). These have been calculated for the times in the tidal cycle corresponding to the spar observations. The region for which $R_i < {}^1/_4$ at some time in the tidal cycle varies between the two broken contours. (c) Temperature difference, ΔT (°C), between the highest and lowest thermistors on the spar.

Fig 12 Observations near 46^o 19' N,.7^o 14' W (150 km from the shelf break in the Bay of Biscay, position B in fig 1) on 5.7.88. (a) isotherms from the XBT survey; (b) Northerly velocities (cm s^{-1}) from the ADCP, relative to the average over 100-200 m; (c) vertical velocities (cm s^{-1}) from the ADCP, relative to the sea surface.

Fig. 13 Temperature data from the IOSDL thermistor spar on 29.4.88 showing two crossings of the Iceland-Faeroes front (a) near the Western side of the front (12°W) and (b) further to the East (at about 11°W). The temperature scale is correct for the top thermistor, each being successively offset by 1°C thereafter.

Fig. 14 A comparison of shear (velocity difference between 18-154 m) along the ship's track from Discovery cruises 181 (ADCP pod retracted, circles) and 164 (pod extended, crosses), with the estimating function E, showing that shear is, for the same severity of conditions as measured by E, on the average much lower with the pod extended.

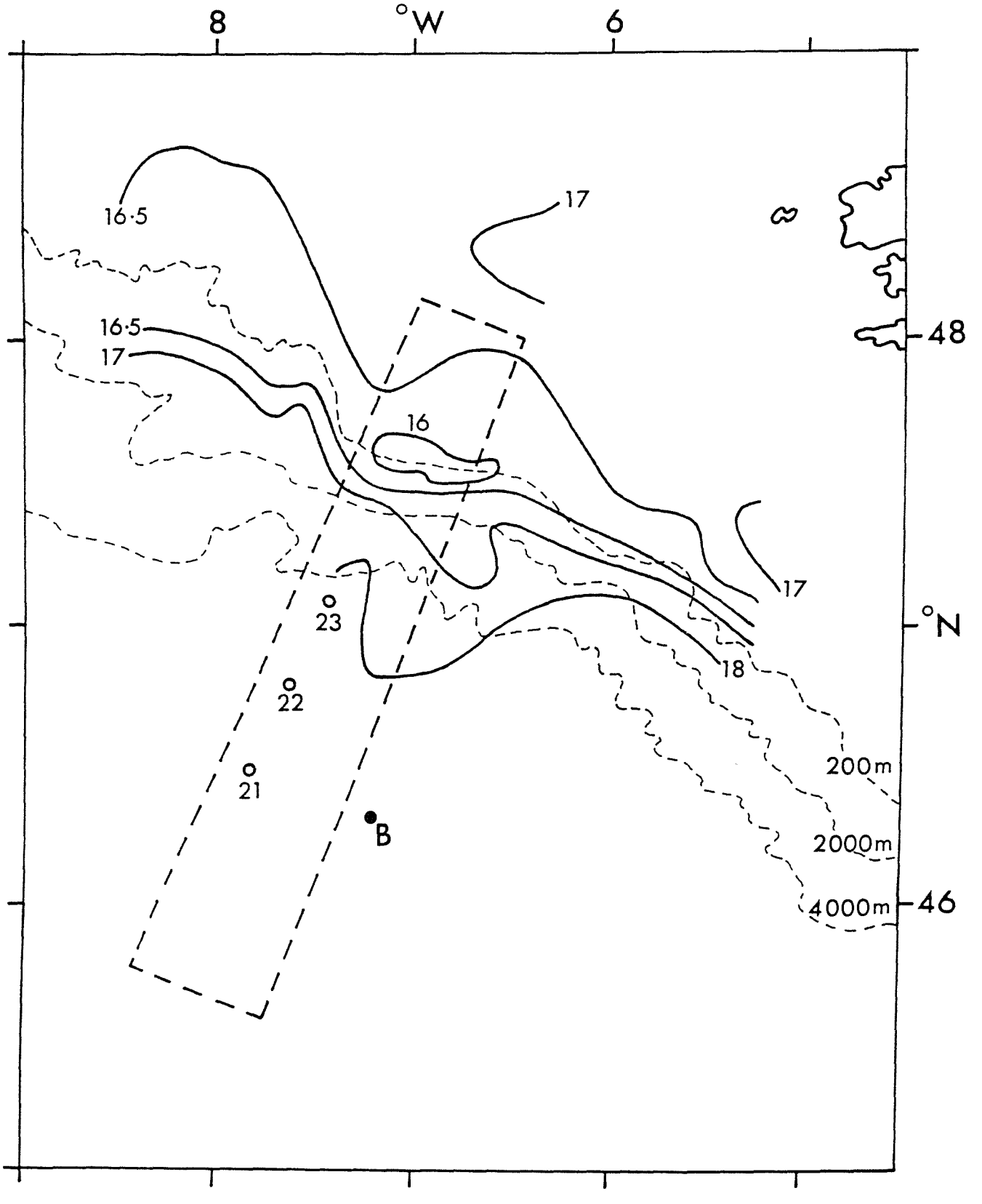

Figure 1

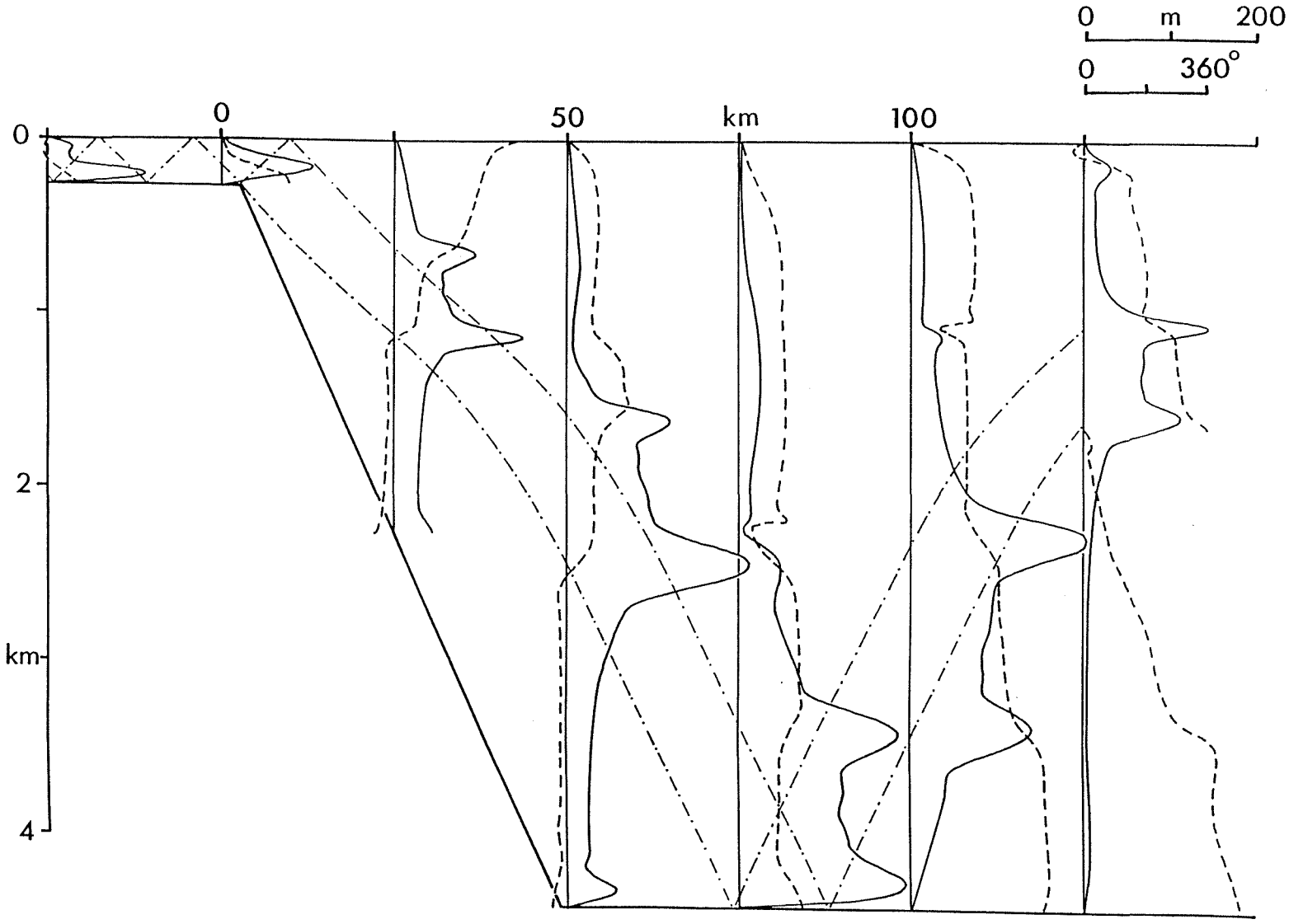

Figure 2

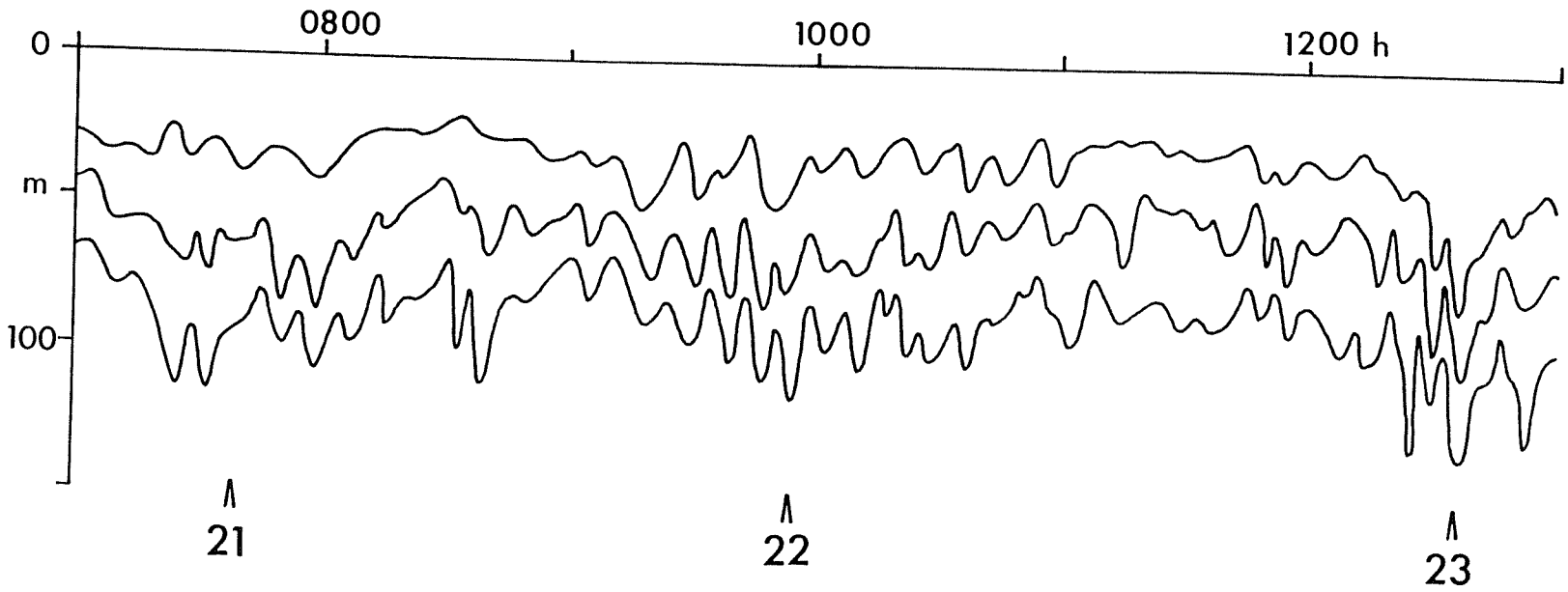

Figure 3

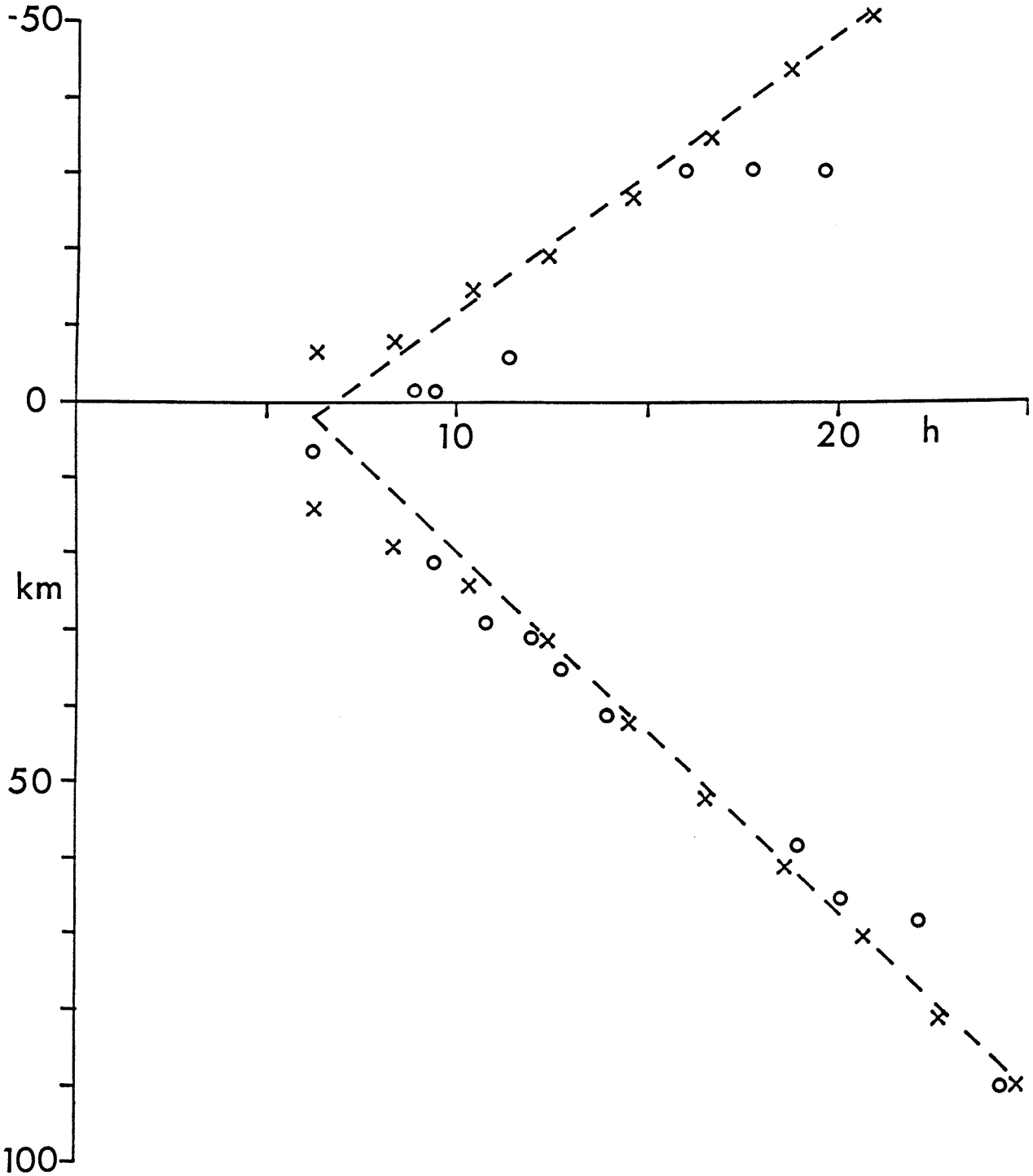

Figure 4

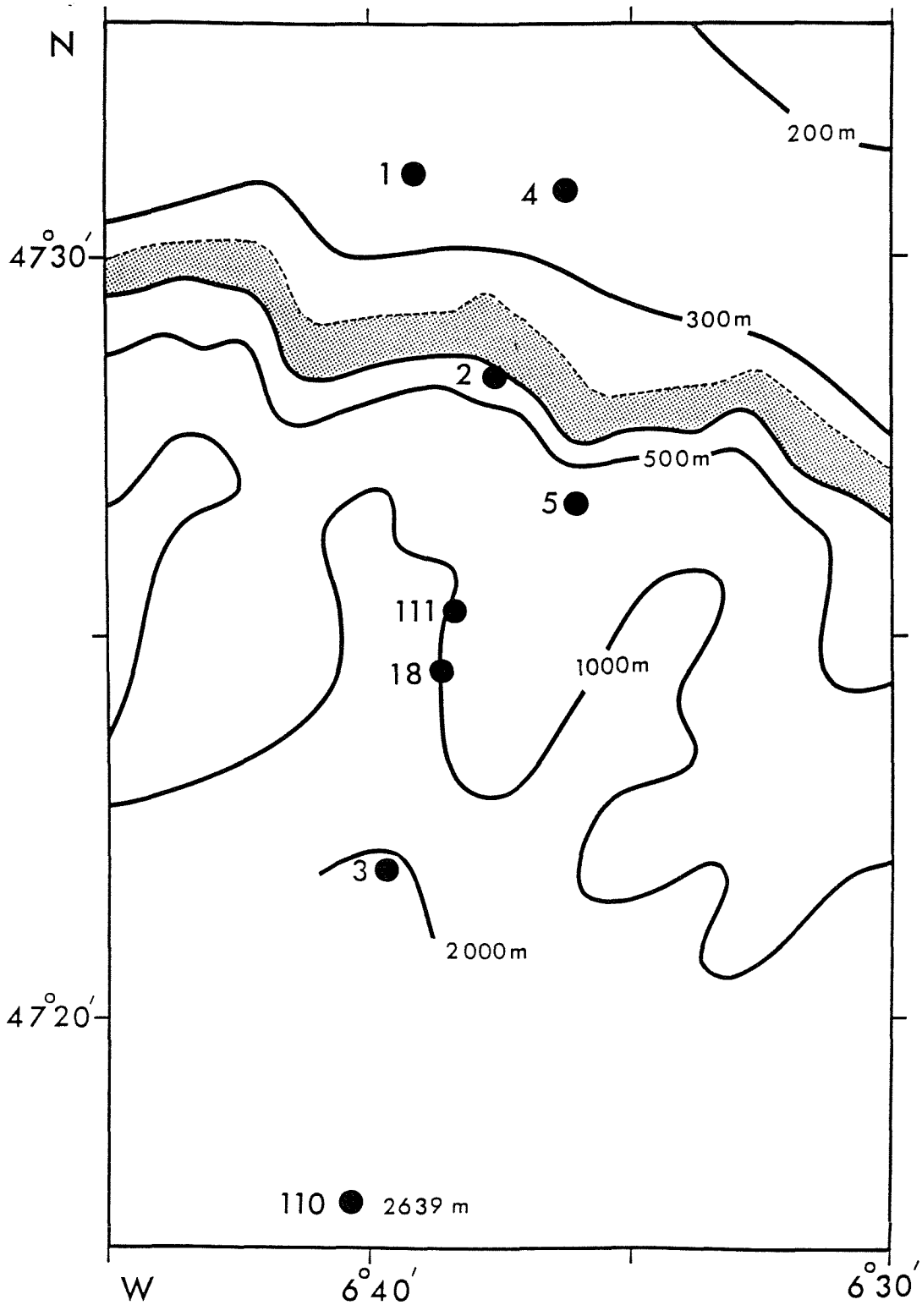
N
200m
1
4
47°30′
300m
2
500m
5
111
18
1000m
3
2000m
47°20′
110
2639 m
W
6°40′
6°30′

Figure 5

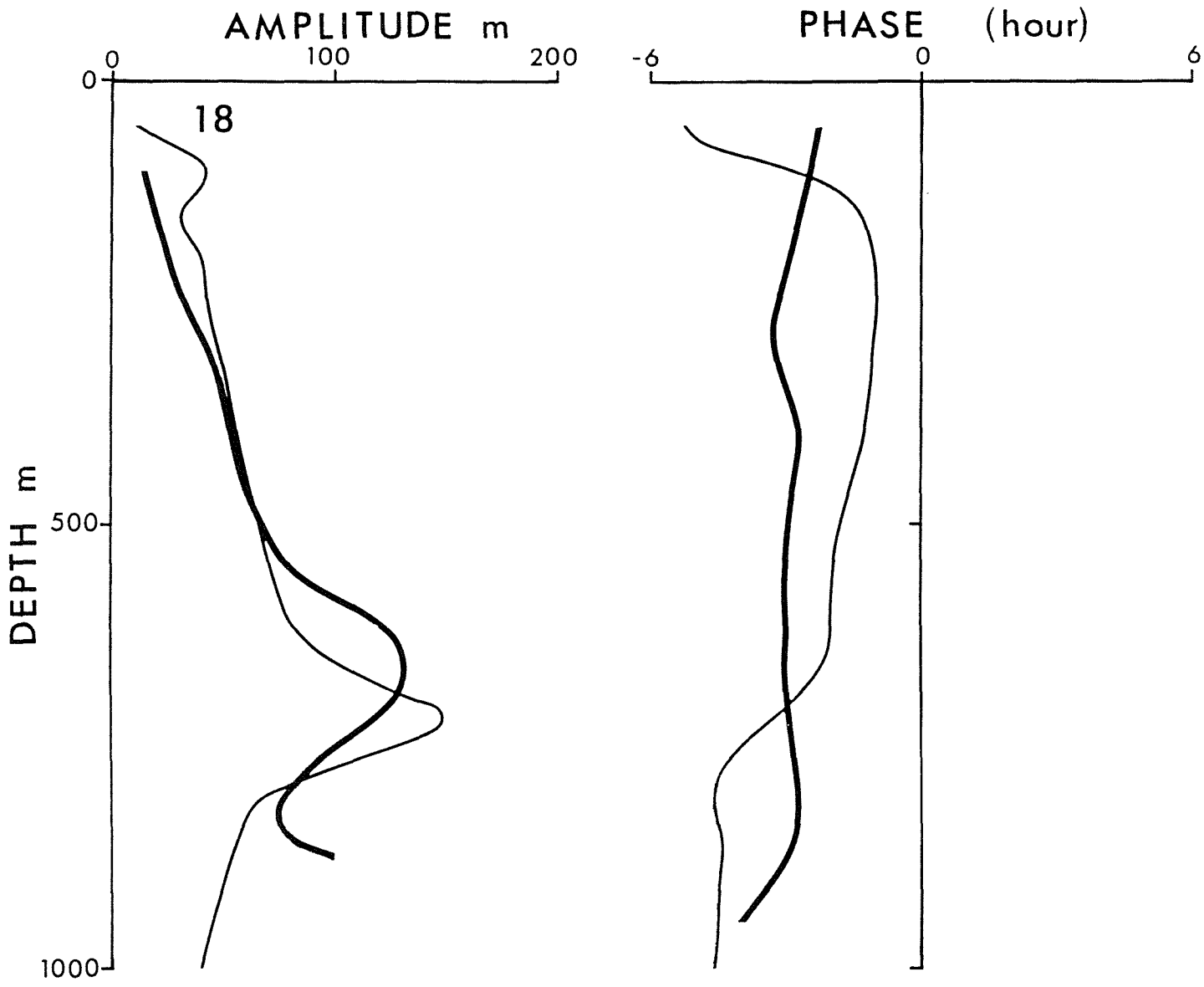

Figure 6

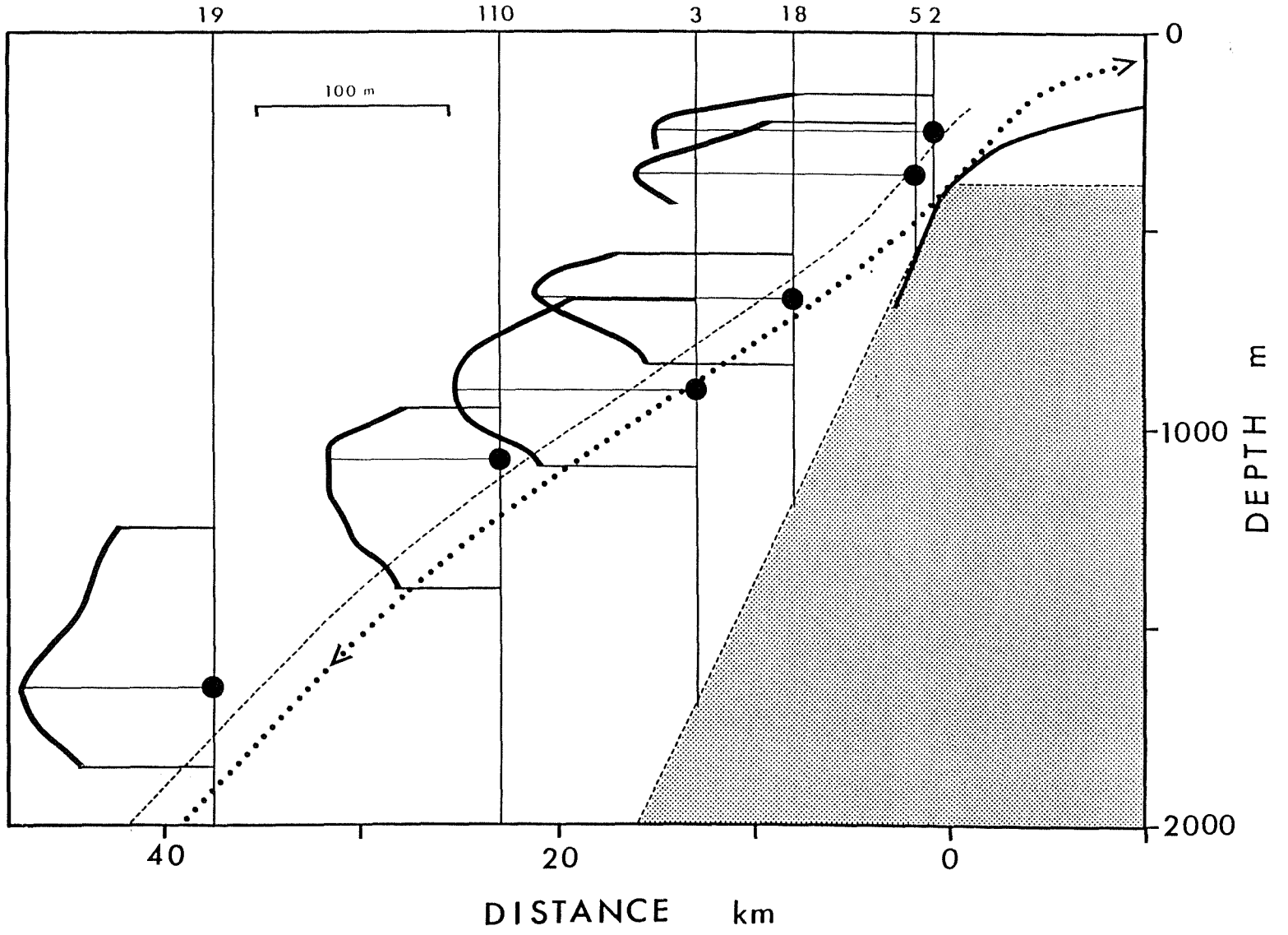

Figure 7

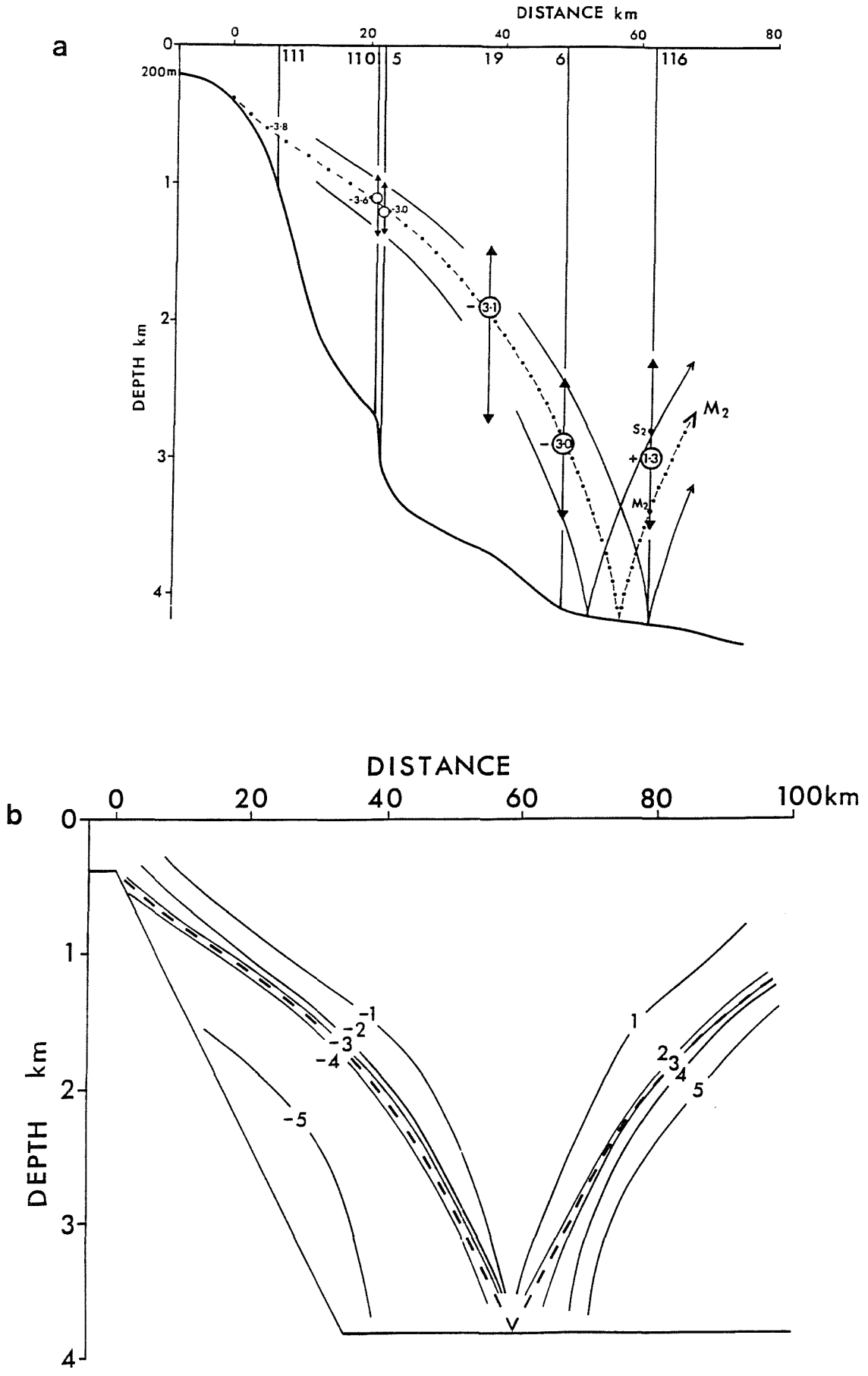
a
DISTANCE km
0
20
40
60
80
111
110
5
19
6
116
200m
1
2
3
4
DEPTH km
-3·8
-3·6
-3·0
-3·1
-3·0
1·3
S2
M2
M2
b
DISTANCE
0
20
40
60
80
100km
DEPTH km
-1
-2
-3
-4
-5
1
2
3
4
5
V

Figure 8

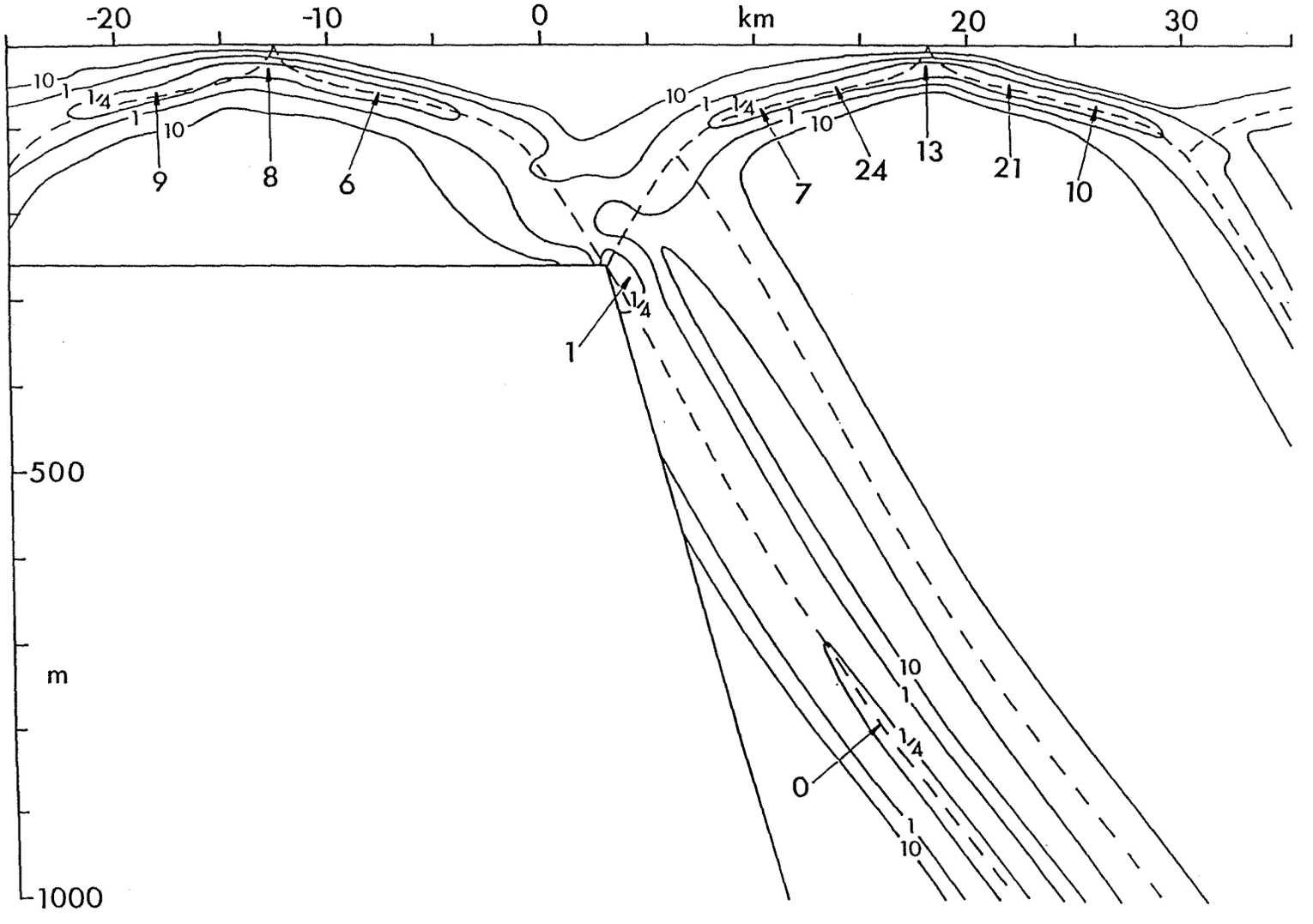
-20
-10
0
km
20
30
10
1
1/4
1
10
9
8
6
10
1
1/4
1
10
7
24
13
21
10
1/4
1
500
m
1000
10
1
1/4
0
1
10

Figure 9

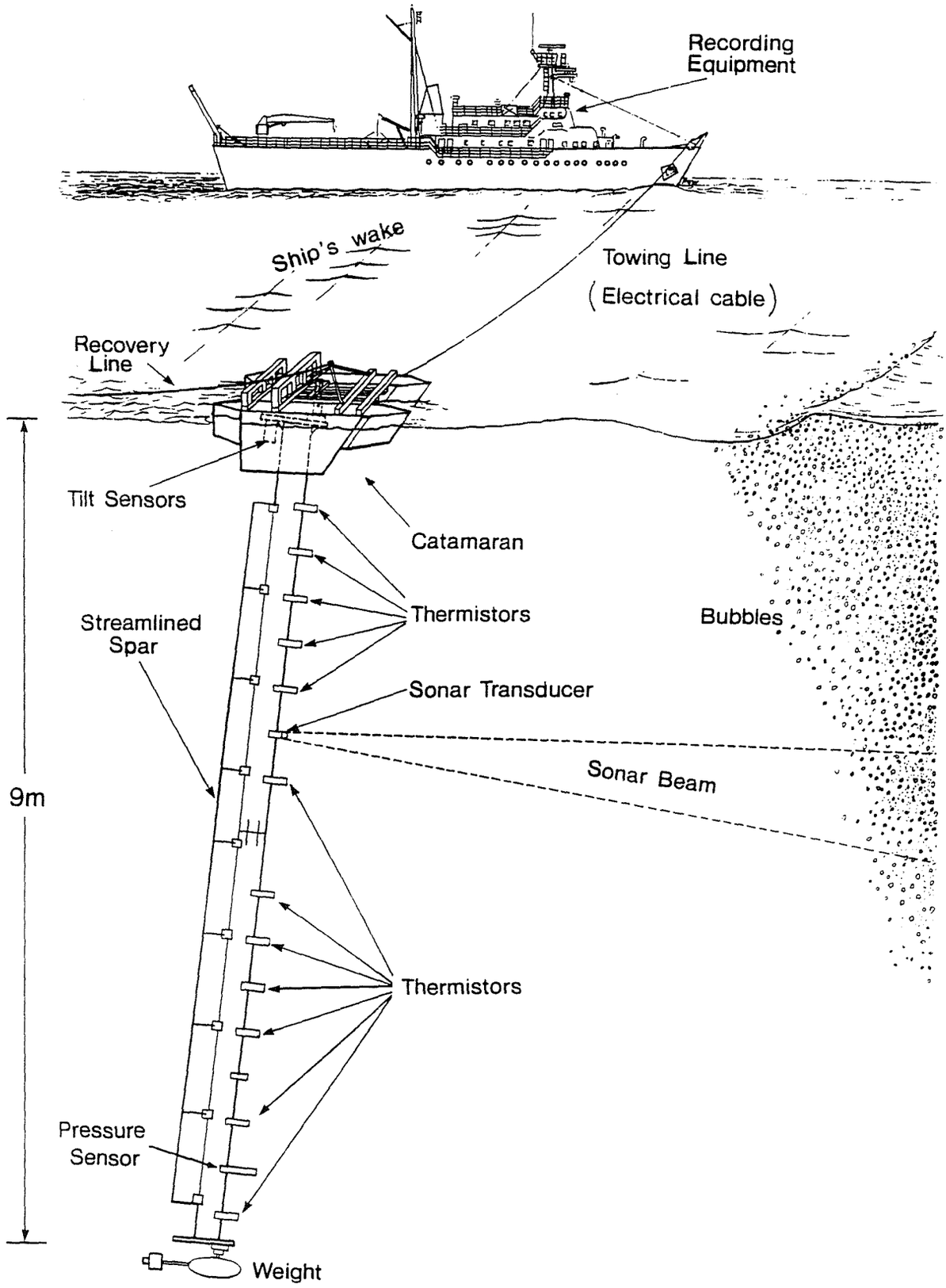
Recording Equipment
Ship's wake
Towing Line
(Electrical cable)
Recovery Line
Tilt Sensors
Catamaran
Thermistors
Bubbles
Streamlined Spar
Sonar Transducer
Sonar Beam
9m
Thermistors
Pressure Sensor
Weight

Figure 10

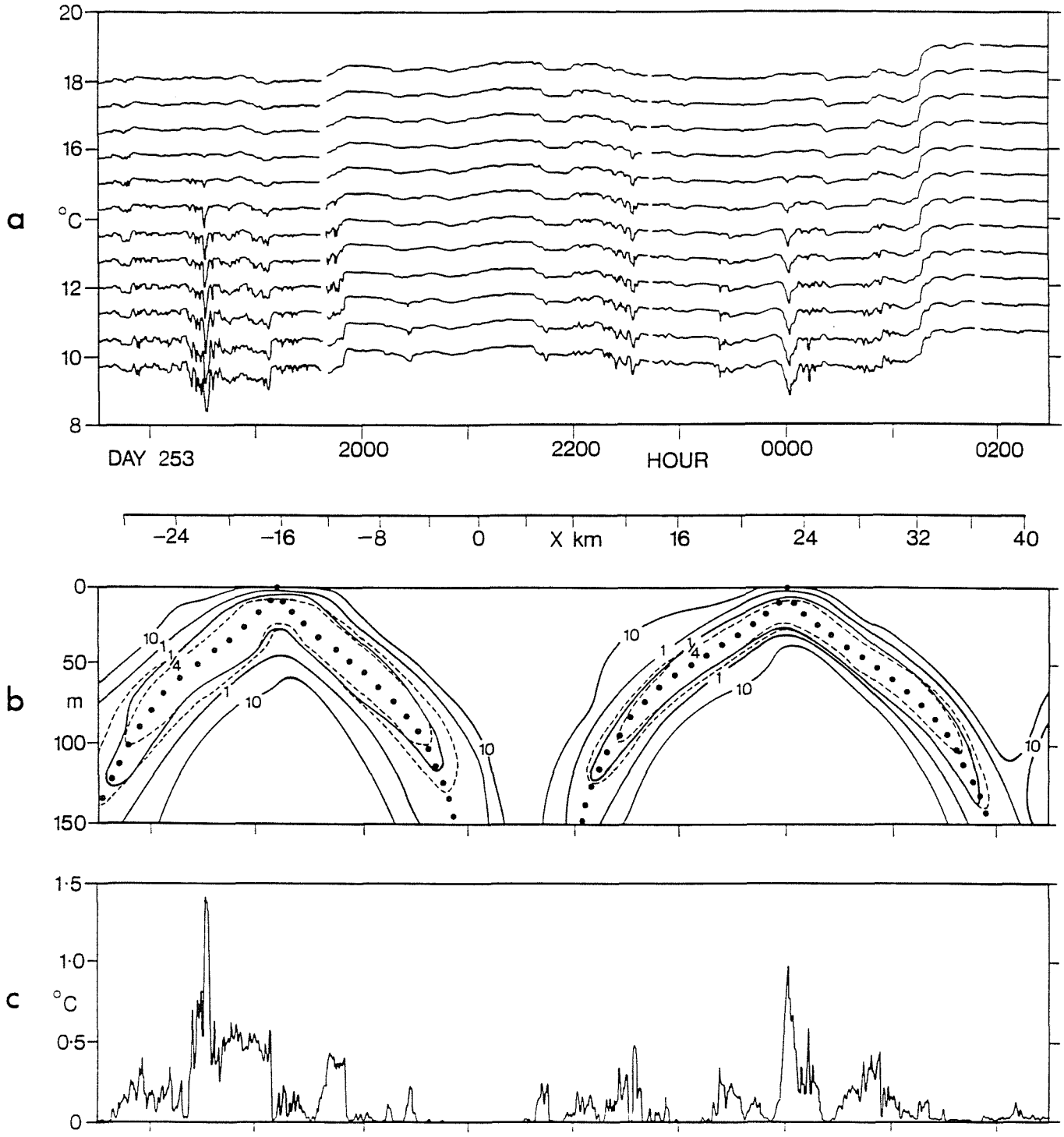
a
20
18
16
°C
12
10
8
DAY 253
2000
2200
HOUR
0000
0200
−24
−16
−8
0
X km
16
24
32
40
b
0
50
m
100
150
10
1
¼
c
1·5
1·0
°C
0·5
0

Figure 11

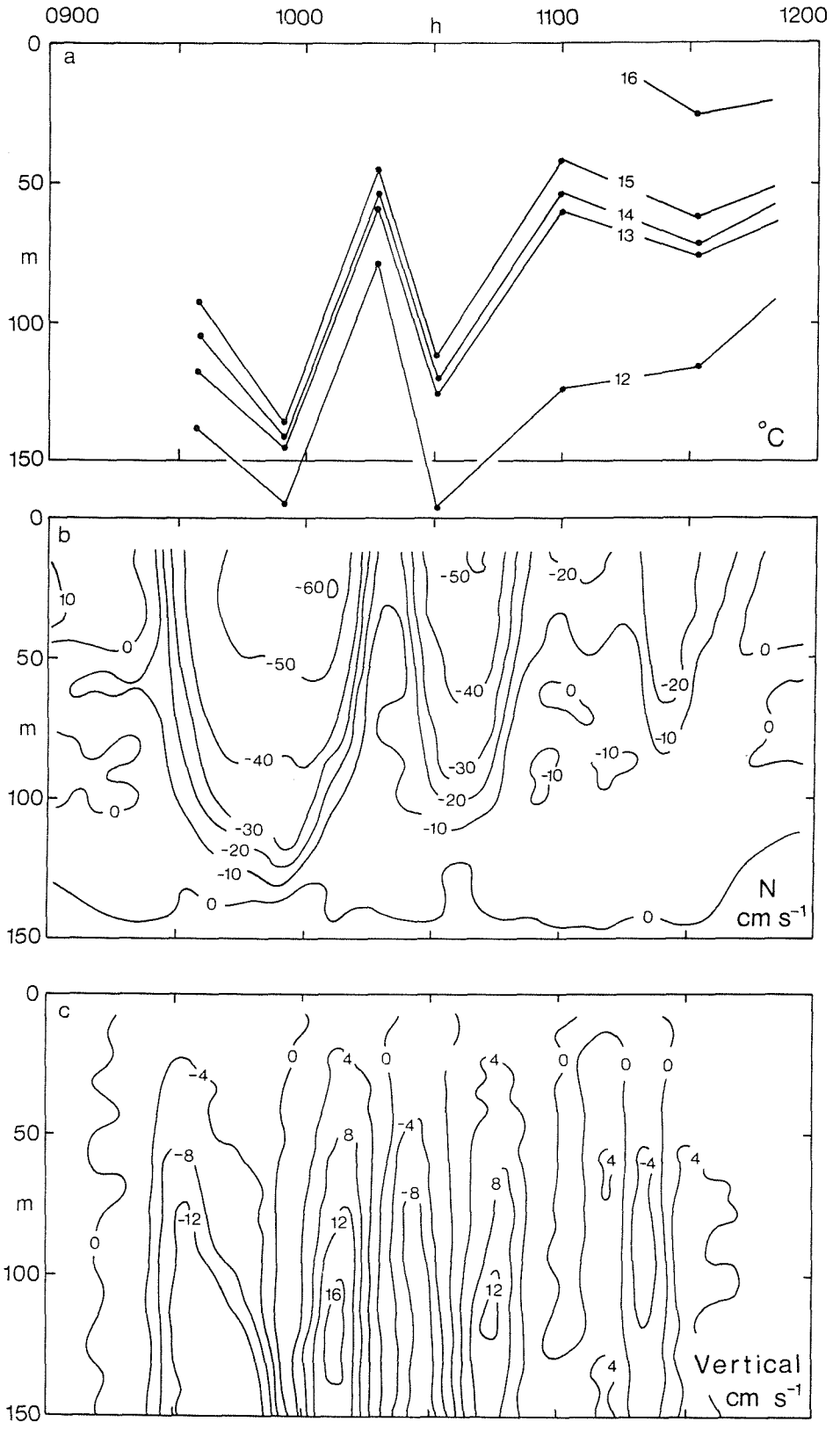
0900
1000
h
1100
1200
a
16
15
14
13
12
°C
b
N
cm s⁻¹
c
Vertical
cm s⁻¹
0
50
m
100
150

Figure 12

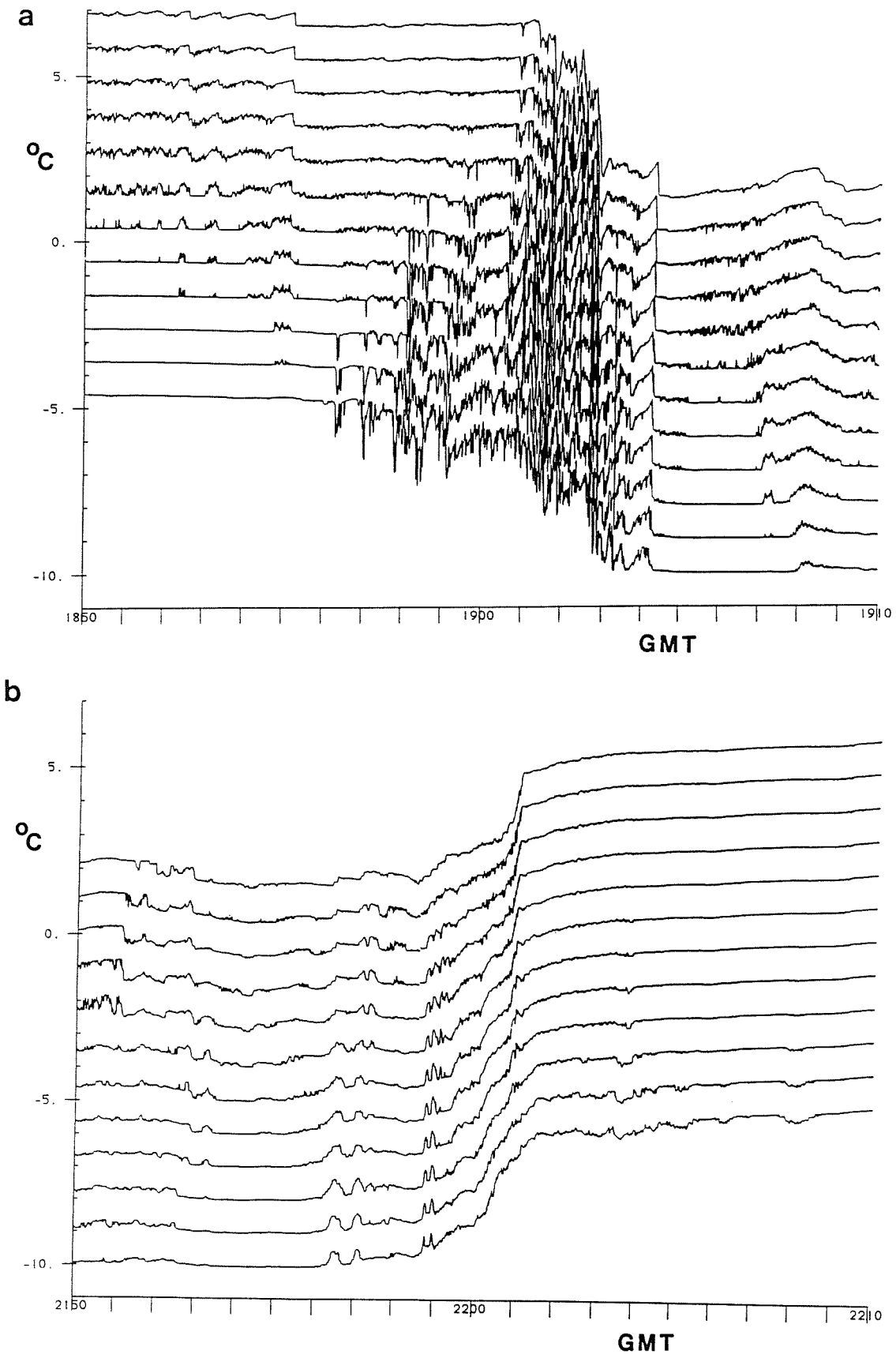

Figure 13

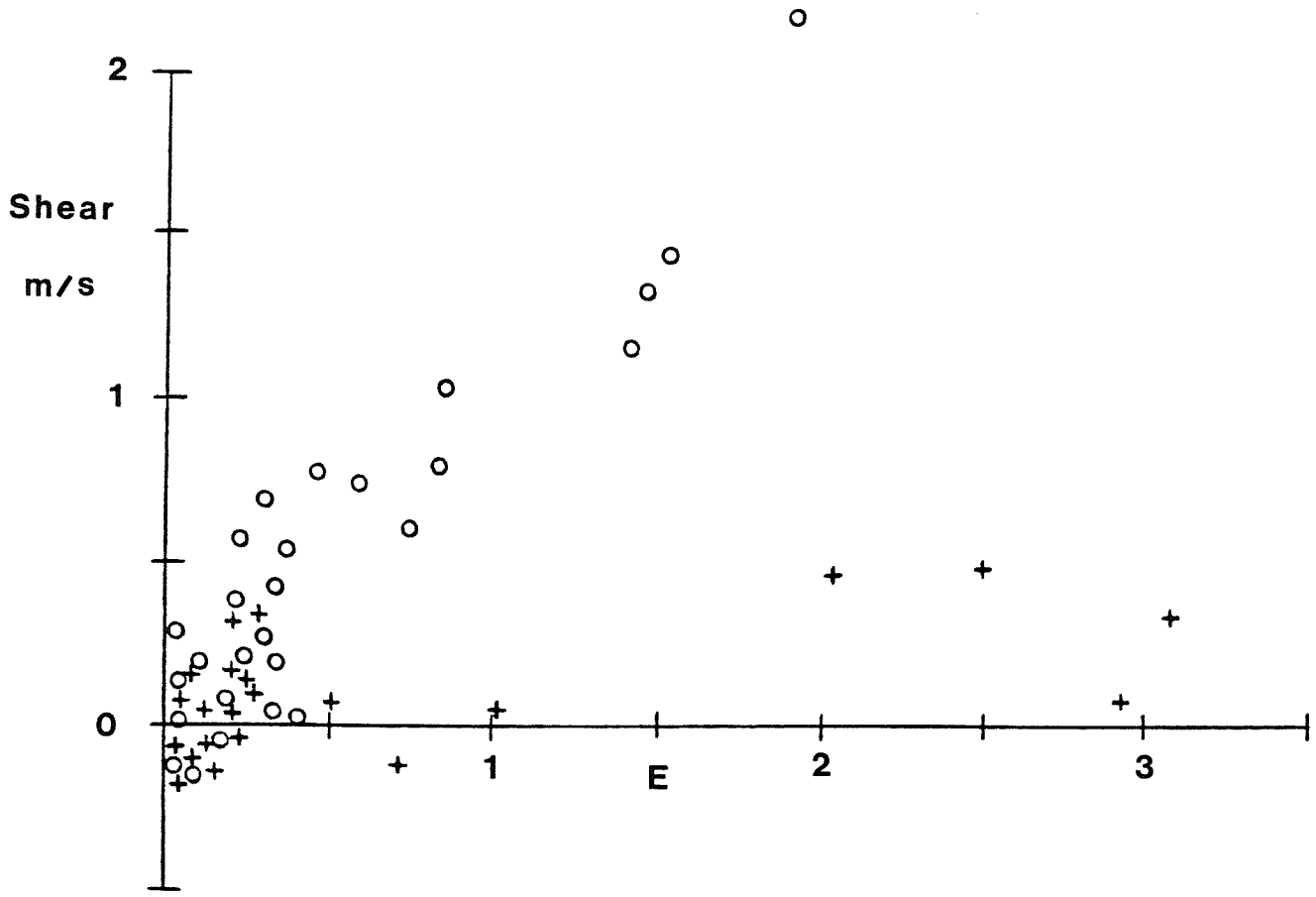

Figure 14